9th International Kimberlite Conference Extended Abstract No. 9IKC-A-00289, 2008

Metasomatism and metamorphism during serpentinisation of the B/K9 Kimberlite, Orapa, Botswana

John Schumacher[1] , Ben Buse[1], Steve Sparks[1], Matthew Field[2]
[1]*Department of Earth Sciences, University of Bristol, Bristol, UK*
[2]*De Beers Group Services, Mendip Court, Bath Road, Wells, UK*

Introduction

The B/K9 kimberlite is situated 15 km east of Orapa in north-central Botswana and is part of a group of over 50 kimberlite pipes (Field *et al.*, 1997) found in the region. During the Cretaceous, the kimberlite was emplaced into the Karoo Supergroup (Field *et al.*, 1997), which consists of mudstones (Tlapana & Tlhabala Formations) overlain by sandstones (Ntane Formation) and basalt (Stormberg Formation). The B/K9 kimberlite is a composite body that consists of three pipes, which separate at depth. The north and south pipes consist of coherent kimberlite (CK). In the central pipe of the kimberlite is overlain by epiclastic deposits.

Petrography of the kimberlite

In the kimberlite, the most prominent textures are the patches of serpentine that replace olivine (up to 10 mm across). In addition to ubiquitous examples of olivine replaced only by serpentine, our preliminary data indicate that in more central parts of the pipe, locally apatite may precipitate with the serpentine of olivine pseudomorphs. Similar textures have been described by Stripp *et al*. (2006) from the Venitia kimberlite pipe The occurrence of apatite suggests that in places the fluids were P-bearing, and that the serpentine-replacement reaction of the olivine drove the pH of the local fluid to high values, which would cause apatite to precipitate. Nearer to the edge of the pipe, some olivine pseudomorphs have calcite cores that are mantled by serpentine. The same mineral assemblages that form the olivine pseudomorphs may also be found in irregularly-shaped patches that may be void filings. Where these irregular serpentine patches show compositional and mineralogical zoning, the olivine pseudomorphs show the same zonation. In these examples, lizardite cores of the patches are altered at very late stages of hydrothermal alteration to a mixture of saponite and lizardite. The lizardite itself shows consistent zoning with slight increases in Al and Fe towards margins of the serpentine patches, which probably reflects a slight temperature decrease during the growth of the lizardite.

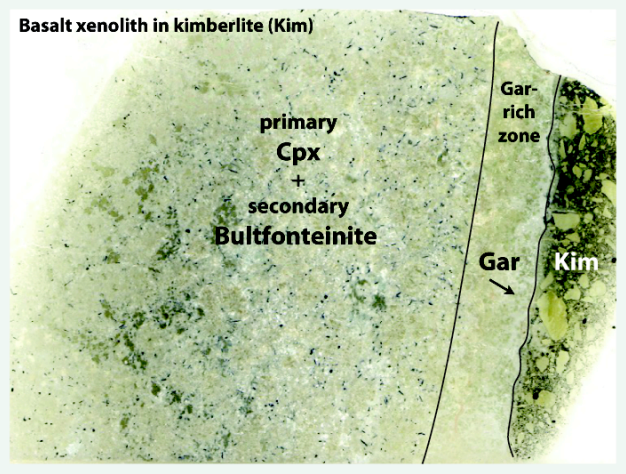

Fig. 1 Sawed section through a basalt xenolith from B/K9 showing a reaction zone at one contact with the kimberlite matrix. *Abbreviations*: Cpx=clinopyroxene; Gar=garnet; Kim=kimberlite. Width of the bottom edge of sample is 3 cm.

Petrography of the basalt inclusions

Field studies show that reaction zones (Fig. 1) are absent or more poorly developed in basalt xenoliths closer to the kimberlite margins, which strongly suggests that the low-T, low-P metamorphism of the xenoliths is related to the hydration and cooling that accompanied the emplacement of the kimberlite. Relict ophitic texture of the xenoliths is obscured at the margins by metasomatic reaction rims, which consist of serpentine and fine-grained (c. 0.1mm across) hydroandradite-hydrogrossular (Ca-Fe^{3+}-Al garnets) (Fig. 1). These garnet compositions are either Al-rich hydrogrossular or spongy-textured and Ti-rich hydroandradite. Ilmenite is ubiquitous throughout the xenolith, except for the zone that is adjacent to the rim, where ilmenite is no longer present and the Ti-bearing hydrogarnets grew.

In the central parts of the xenoliths, the rare mineral, bultfonteinite with an ideal formula of $Ca_2SiO_2(OH)_3F$, forms pseudomorphs after plagioclase. The (OH)-F ratio in bultfonteinite is variable, and, in fact, F-free bultfonteinite is known. However, all the bultfonteinite currently found at B/K9 has near ideal F contents, but F

can vary up to about 10% from ideal values. The bultfonteinite itself is partially replaced by later growth of very fine-grained hydrogarnet that nucleated in fractures (Fig. 2). Clinopyroxene is present throughout the xenolith and shows some replacement by bultfonteinite and serpentine. The bultfonteinite that replaces clinopyroxene, like the bultfonteinite found in the plagioclase pseudomorphs, also shows minor replacement by hydrogarnet (Fig. 2). This xenolith also contains serpentinized patches, which may have

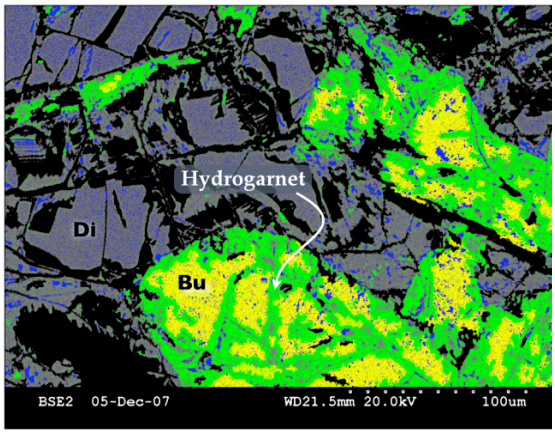

Fig. 2 Back scatter image that has been enhanced with color that shows the distribution of clinopyroxene (Di, gray-blue), bultfonteinite (Bu, yellow) and hydrogarnet (green) that replaces the bultfonteinite.

formed from altered volcanic glass. These patches are now partially replaced by amorphous hydrogarnet and bultfonteinite, and, near the rim, and larger subhedral hydrogarnets grow within these serpentinized patches (Fig. 1).

Phase relations

The T-X_{CO2} stability field of bultfonteinite is not well known, but some inferences can be made. In the relatively simple system CaO-SiO_2-fluid (H_2O-CO_2), wollastonite and xonotlite [$Ca_6Si_6O_{17}(OH)_2$] are less hydrated and carbonated solid phases that are compositionally equivalent to F-free bultfonteinite [$Ca_2SiO_2(OH)_4$] + calcite. Wollastonite, which is H_2O-CO_2 free, would have the largest stability field. Xonotlite is more hydrated than wollastonite, but less hydrated and carbonated than the bultfonteinite + calcite assemblage and would be expected to have a T-X_{CO2} stability field that is wider than bultfonteinite, but less extensive than wollastonite. Reactions like:

(1) SiO_2 + xonotlite + H_2O + F = bultfonteinite, and
(2) SiO_2 + calcite + H_2O + F = bultfonteinite + CO_2

should constrain P-T-X_{CO2} stability of bultfonteinite. The approximate stability field can be estimated from using experimentally-determined and calculated equilibria in combination with Schreinemaker's analysis (Fig. 3). Bultfonteinite is expected to be stabile in the presence of water-rich fluids. Obviously, the natural compositions indicate fluorine must also be present, but work by Tropper and Manning (2007) suggest at temperatures below 600°C the concentration of fluorine in the fluid phase is likely to be below 17 ppm (based on solubility of fluorite). These fluorine concentrations are not enough to perturb the T-X_{CO2} relations.

The assemblages of the serpentinized kimberlite also constrain the X_{CO2} composition of the pervading fluid. The common assemblage at B/K9 is serpentine (lizardite) + calcite, which has an upper thermal stability of almost 390°C with and X_{CO2} values up to about 0.2 at the highest temperatures (Fig. 3); however, the maximum X_{CO2} values decrease greatly with even small reductions in temperature. Together, these data suggest that the stability field of bultfonteinite is probably in the range of 350-250°C with a very water-rich attending fluid phase (probably $X_{CO2} < 0.05$).

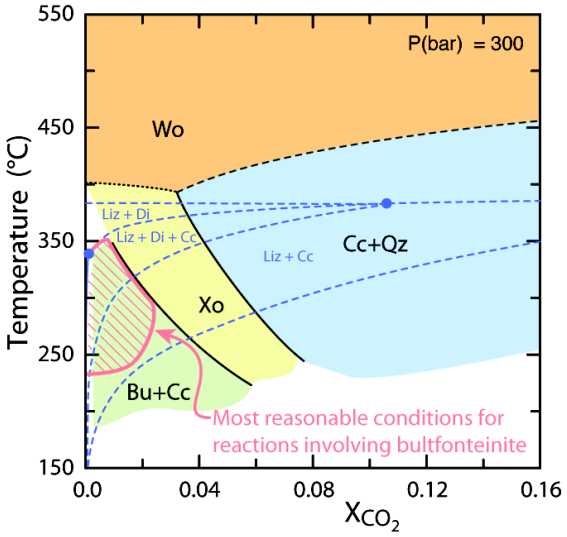

Fig. 3 T-X_{CO2} diagram showing the estimated stability region of bultfonteinite (Bu) with the stability fields for assemblages in the serpentinized kimberlite superimposed (dashed blue lines). Dashed lines are calculated with Perplex (Connolly, 2005); dotted line is based on experimental stability of xonotlite (Pistorius, 1963); solid lines are estimated from positions of the other equilibria. *Other abbreviations*: calcite (Cc), diopside (Di), lizardite (Liz), quartz (Qz) and wollastonite (Wo).

Metasomatic growth, advective transport and cooling

The textures described above suggest the growth of lizardite, bultfonteinite and hydrogarnet were partly driven by chemical-potential gradients for SiO_2, Al_2O_3 and CaO that are concentrated in the basalt and H_2O and MgO that are concentrated in the kimberlite. However, the actual mechanism leading to these textures is likely to involve both diffusional and advective transport of material. The mineralogical

zoning in the xenoliths (Fig. 1) probably represents textures that developed at higher temperatures where diffusion is more effective. The presence of relict clinopyroxene, for example is evidence that the gradients for SiO_2, CaO, H_2O and MgO were still intact until the relevant and dominantly diffusion-controlled reactions shutdown due to cooling. The partial replacement of initial metamorphic assemblage (*e.g.*, bultfonteinite by hydrogarnet, Fig. 2) along fractures suggest advective transport of material was the dominant mechanism of mineral growth at these, probably lower temperature, conditions.

One surprising observation is that the complete replacement of plagioclase by bultfonteinite suggests that Al_2O_3, normally considered to be relatively immobile, was completely dissolved, and subsequently precipitated as the hydrogarnet partially replaced the bultfonteinite.

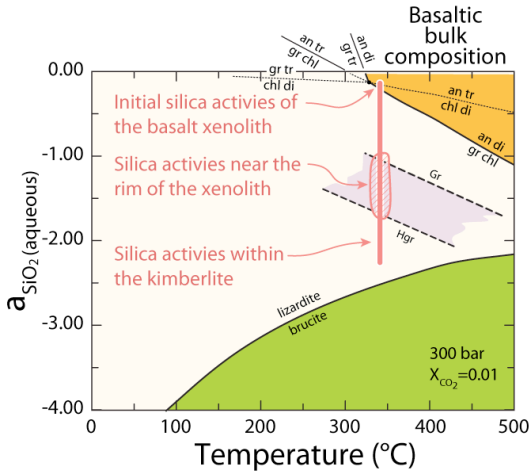

Fig. 4 Temperature-a_{SiO2} diagram after Frost and Beard (2007) that shows the best estimated conditions for hydrogrossular (Hgr) growth by diffusional growth process. End member equilibria are calculated with Perplex (Connolly, 2005). *Other abbreviations*: anorthite (an), chlorite (chl), diopside (Di), grossular (gr) and tremolite (tr).

The activity of aqueous silica can be estimated from activity-temperature diagrams. Assuming the presence of sufficient Al in solution, Figure 4 can be used to estimate the conditions of formation for the hydrogrossular based on the stability of end-member phases on the T-a_{SiO2} diagram. The conditions for hydrogarnet growth are in good agreement with the estimates from the bultfonteinite (Fig. 3) suggesting that these reactions occurred between about 250 and 350°C at P < 500 bars in the presence of an extremely water-rich fluid that was undersaturated (minus one to two log units) in SiO_2.

Acknowledgments

Ben Buse is supported by a NERC-CASE studentship awarded at the University of Bristol.

References

Connolly, J.A.D. (2005). Computation of phase equilibria by linear programming: A tool for geodynamic modeling and its application to subduction zone decarbonation. Earth and Planetary Science Letters 236, 524-541.

Field M., Gibson J.G., Wilkes T.A., Gababotse J. and Khutjwe P. (1997) 'The geology of the Orapa A/K1 kimberlite Botswana: Further insight into the emplacement of kimberlite pipes'. Russian Geology and Geophysics 38, pp 24-39.

Frost, B.R. and J.S.Beard (2007) On Silica Activity and Serpentinization. *Journal of Petrology* 48, 1351-1368.

Pistorius, C.F.T. (1963) Thermal decomposition of portlandite and xonootlite to high pressures and temperatures. *American Jornal of Science* 261, 79-87.

Stripp, G.R., M. Field, J.C. Schumacher, R.S.J. Sparks and G. Cressey (2006) Post-emplacement serpentinization and related hydrothermal metamorphism in a kimberlite from Venetia, South Africa. *Journal of Metamorphic Geology* 24, 515-534.

Tropper, P. and C.E. Manning (2007) The solubility of fluorite in H_2O and H_2O–NaCl at high pressure and temperature. *Chemical Geology* 242, 299–306.